

NISS

Water Permeability of Cracked High Strength Concrete

Corina-Maria Aldea, Surendra P. Shah,
and Alan F. Karr

Technical Report Number 77
March, 1998

National Institute of Statistical Sciences
19 T. W. Alexander Drive
PO Box 14006
Research Triangle Park, NC 27709-4006
www.niss.org

Water Permeability of Cracked High Strength Concrete

By Corina-Maria Aldea, Surendra P. Shah and Alan Karr

Synopsis: The goal of the research presented here was to study the relationship between cracking and water permeability. A feedback-controlled test was used to generate width-controlled cracks and then water permeability was evaluated by a low-pressure water permeability test. The factors chosen for the experimental design were: material type, thickness of the sample and average width of the induced cracks. The water permeability test results indicated that the relationships between permeability and material type differ for uncracked and cracked material. Permeability of uncracked material decreased from paste, mortar, normal strength concrete (NSC) to high strength concrete (HSC), as expected. However, for cracks above 100 microns, NSC showed the highest permeability coefficient. Water permeability of cracked material increased with increasing crack width, material type had effect on permeability and there was little thickness effect. HSC behavior in terms of crack recovery and permeability for cracks above 100 microns ranged between mortar and normal strength concrete.

Keywords: cracks, crack width, crack opening displacement (COD), cumulative flow, damage, feedback-controlled test, permeability coefficient, recovery, splitting tensile test, water permeability.

Corina-Maria Aldea is a post doctoral research fellow at the Center for Advanced Cement-Based Materials, Northwestern University. She received her Ph.D. from the Technical University of Civil Engineering, Bucharest, Romania. She has been

involved with research on hydraulic structures, space structures, fiber reinforced concrete and durability of concrete.

Surendra P. Shah is a Walter P. Murphy Professor of Civil Engineering and Director of the NSF Center for Advanced Cement-Based Materials at Northwestern University. In addition to co-authoring three books, he has edited 12 books, and published over 400 technical papers. He is Editor-in-Chief of Advanced Cement Based Materials and has received numerous awards and honors from institutions throughout the world.

Alan F. Karr is Associate Director of the National Institute of Statistical Sciences and Professor of Statistics and Biostatistics at the University of North Carolina at Chapel Hill. His research interests lie at the cross-disciplinary interfaces of statistics with other fields, including materials science, software engineering and computer science.

INTRODUCTION

Concrete permeability plays a critical role in controlling the properties of concrete and the performance of concrete structures. In particular durability of concrete and the corrosion of reinforcing steel are intimately linked to the water permeability of exposed concrete surfaces. Whereas the beneficial effects of high strength concrete on load capacity of concrete structures are relatively well established, knowledge concerning serviceability, and particularly concerning cracking is scarce. Cracking behavior is important with regard to durability requirements, as cracks that may form, whatever their origin, can act as major pathways for water or aggressive chemical ions to penetrate in concrete, enabling its deterioration.

Results from permeability studies on cracked concrete showed dependence of permeability on crack widths. A prior permeability study performed at ACBM, Northwestern University introducing feedback-controlled splitting tests to induce width-controlled cracks in normal strength concrete specimens was reported earlier and pointed out the advantages of using feedback-controlled splitting tests to obtain a series of specimens with crack widths ranging from 25 to 550 microns [2]. Water permeability proved dependent on the value of the crack opening in the concrete. Gerard et al. [4], [5] studied the increase in permeability resulting from mechanically-induced cracking for normal and high concrete. Samples were subjected to uniaxial tension, and the water permeability was measured in a direction perpendicular to the axis of loading through open cracks having widths ranging from 0.1 to 100 microns. The experimental results showed that the permeability of the specimens is strongly dependent upon the crack width.

Based on the conclusions pointed out by [2], the present study focuses on the relationship between cracking and concrete permeability and is novel by the experimental design and the parameters considered [1]. The experimental design included factors such as: material type (paste, mortar, normal strength concrete and high strength concrete), thickness of the sample (25 and 50 mm), and average width of the induced cracks (ranging from 50 to 350 microns). Feedback controlled splitting tensile test was used to induce microcracks of designed widths in the concrete specimens. Water permeability of cracked samples was then evaluated by the low pressure water permeability test. Results suggest that among the considered parameters material type and crack parameters affect water permeability. The results of the present study can be used in a design phase of a structure or in the repairs of crack formation in existing construction.

EXPERIMENTAL PROGRAM

Test Series and Mixture Proportions

Details of mixture ingredients and their proportions are presented in Table 1 and material properties in Table 2. Test series included (1) paste (PASTE), (2) mortar (MORTAR), (3) normal strength concrete (NSC), with a water to cement ratio $w/c=0.45$, and (4) high strength concrete (HSC), with $w/c=0.31$. Cylindrical molds 10 x 20 cm (4 x 8 in) were used for casting. Cylinders were demolded after 24 hours and then stored in a controlled chamber, at 20° C and 100% RH until the age of 28 days. Cylinders were sawn into slices, and then tested. Middle slices were used for testing. Samples were soaked in water at room temperature immediately after cutting, as well as in between the tests, in order to avoid drying and any further microcracking. Cutting was performed a day before inducing cracks by means of the feedback-controlled splitting test. Then cracked samples were vacuum saturated according to C1202-94 [6] and set up for the water permeability test (WPT).

Feedback-controlled Test

Feedback-controlled splitting tests were used to induce width-controlled cracks in the specimens (Fig. 1). Splitting tensile test is one of the methods for estimating the tensile strength of concrete through indirect tension tests [7]. This test was carried out on cylindrical samples, 10 cm (4 in) diameter and 25 mm or 50 mm (1 in or 2 in) thick, tested on their side in diametral compression. Load was applied through narrow bearing plywood strips (25 mm wide and 3 mm thick), interposed between the cylinder and the platens of the testing machine.

The 4.4 MN (one million pound) test machine with a 490 kN strain gage load cell to measure the force was used for the tests. Force calibrated range was

different, depending to the test series: HSC required a higher range (489 kN), while as for the rest of the tested materials a lower range (49 kN) was used. As crack rarely propagates simultaneously from both sides of the cylinder when under load, the displacement was monitored on both sides of the specimen with two transducers, and the controlled variable was the average recorded displacement of the two LVDTs [8]. One linear variable displacement transducer (LVDT) with a range of 0.5 mm was glued on each side of the slices, normal to the loading direction. Specimens were loaded under the feedback controlled condition until the average crack reached the desired imposed value, then unloading was performed under force control. Imposed crack openings under loading were 50, 100, 140, 170, 200, 250, 300 and 350 microns. As PASTE proved very brittle and extremely difficult to test; the maximum crack opening introduced under loading was limited to 200 microns. Test results were plotted as individual stress versus COD curves for all the slices tested.

Water Permeability Test

Cracked samples were used for the water permeability test, involving: vacuuming and saturation, setting up the test and taking the measurements, as described in [2].

Vacuuming and saturation were performed according to the sample preparation suggested for the rapid chloride permeability test [8]. Once removed from the desiccator, the discs were clamped in the water permeability test setup, according to the procedure described in (1). A pipette (10 ml x 1/10) was mounted in the top plate in order to monitor the water level, and a U-shaped copper pipe was mounted on the bottom plate, in order to ensure the atmospheric pressure at the bottom level of the sample.

Water permeability test (WPT) represents a modified version [2] of a water permeability test developed at the University of Illinois at Urbana-Champaign [3]. It consisted in monitoring the water level in the pipette and then refilling it at the initial level. During the test only inflow was measured. The setup was based on the idea of axial water flow through the sample, due to a low pressure of approximately 30-cm head (Fig. 2). The change in head was recorded regularly, depending on the material type, the average crack opening after unloading, and the time elapsed after the beginning of the test. In the literature testing duration varies between 7 [9] and [10], 15 [3] and 21 days [11] for uncracked normal strength concrete, and 20 days for cracked normal strength concrete [2]. In the present study water permeability was monitored up to 90 to 100 days for all the specimens tested.

In the calculations laminar flow was assumed. Based on Darcy's law used for the flow through the samples:

$$Q = kA \frac{h}{l} \quad (1)$$

and continuity of flow throughout the system [12], the permeability coefficient results:

$$k = \left(\frac{A'l}{At_i} \right) \ln \left(\frac{h_0}{h_i} \right) \quad (2)$$

where: A is the cross sectional area of concrete, A' the area of the pipette, l the thickness of the sample, t_i is the time between two successive readings, h₀, h_i the head of water at the beginning, respectively at the end of the test.

DISCUSSION OF RESULTS

Feedback-controlled Test

Typical stress COD curve for HSC is plotted in Fig. 3. Individual curves exhibited similar trends, and the following can be remarked. The experimental data in the present study confirmed that the crack does not propagate simultaneously from both faces, as stated in [2] and [8]. A linear part corresponds to loading of the specimen up to the peak load, when the tensile strength of the material is reached. Average lateral displacements corresponding to the peak load were about 12 microns for HSC, which were in the range from about 9 microns for PASTE and NSC, to 16 microns for MORTAR. As the tensile strength was reached, cracking was initiated, a drop in load and a plateau of slightly increasing load was noticed. Similar behavior was noticed for MORTAR, while as PASTE and NSC exhibited a plateau of almost constant load. The percentage of the peak load in the plateau was within an average of about 65% for HSC, which compared to the one corresponding to MORTAR, and ranged between about 40% for PASTE and 80% for NSC. The specimen was unloaded as soon as the designed average lateral displacement was reached. After unloading, the crack partly closed, and the widths were reduced to an average of 65% of the opening under loading for HSC. Crack recovery ranged between 32% for NSC and 75% for MORTAR.

Recovery of crack opening displacement after unloading is presented in Fig. 4. Investigating the influence of the geometry of the specimens (Fig. 4), the results suggest that thickness of the samples had little effect upon COD after unloading. HSC had a linear behavior for COD under loading below 200 microns, while as for values above 200 microns it became nonlinear. Thinner specimens exhibited a slightly more pronounced nonlinear behavior. Compared to the tested materials, HSC results ranged between MORTAR, which behaved most linearly, and NSC, which behaved most nonlinearly, especially for the thinner specimens.

Water Permeability Test

Water permeability was quantified in the present study by cumulative flow and permeability coefficient. Cumulative flow curves were plotted based on change in head. Fig. 5 indicates that cumulative flow increases with crack opening. The curves clearly distinguish a nonlinear behavior in the first days of water permeability test and then a linear behavior, proving a steady flow. Some results [3] for uncracked normal strength concrete suggest that the nonlinear part of the curve is due to continued saturation, absorption of water into the interconnected pores, or continued hydration, which take place for about 7 days. Other investigators [11] assume that steady state flow is reached when outflow equals inflow, that is 8 to 21 days after the beginning of the test.

According to [3] the slope of the cumulative flow curve is proportional to the permeability coefficient at any time. The permeability coefficient was calculated as an average of permeability coefficients calculated between day 14 and 20. Fig. 6 presents a typical permeability coefficient curve in time. Each point in the figure represents an individual permeability coefficient based on equation (2) and corresponding to the time frame between two successive readings.

Fig. 7 presents thickness effect on HSC permeability coefficient. Within the cracking range, for COD after unloading below 200 microns, permeability coefficient increases with two orders of magnitude compared to the uncracked material. It can be observed that although permeability coefficients for the considered thicknesses were not identical for uncracked material or almost similar crack widths, they were however comparable. Thus it can be concluded that thickness had little effect on permeability. MORTAR exhibited the least thickness dependence among the presented materials

Fig. 8 and Table 3 present material and cracking effect on permeability in the same cracking range after unloading (about 100 microns). It can be observed that permeability showed dependence on material type. Permeability of uncracked material decreased from PASTE, MORTAR, NSC to HSC, as expected. Cracking changed the material behavior in terms of permeability. For cracks above 100 microns after unloading, NSC showed the highest permeability coefficient, while as MORTAR showed the lowest value. Crack pattern investigation for 25 mm NSC samples [2] showed that secondary cracks as well as additional smaller cracks leading to a network of joined cracks develop with increased loading. Probable presence of secondary cracks, as well as crack connectivity might have increased NSC in the range of wider cracks.

SUMMARY AND CONCLUSIONS

- Results of the feedback-controlled splitting tests indicate that
 - The relationship between COD under loading and COD after unloading for HSC is comparable to all the other materials tested.
 - Thickness of the samples had little effect upon COD after unloading for all the materials tested.
- Results of the water permeability test indicate that:
 - The relationships between permeability and material type differ for uncracked and cracked specimens.
 - Permeability of uncracked material decreased from PASTE, MORTAR, NSC to HSC, as expected.
 - For cracks above 100 microns, NSC showed the highest permeability coefficient, while as MORTAR showed the lowest one.
 - Permeability of cracked material increased with increasing cracking. For cracks close to 100 microns permeability coefficient increased with up to three orders of magnitude compared to that corresponding to uncracked material.
 - Thickness of the samples had little effect upon permeability for all the materials tested.
- HSC behavior in terms of crack recovery and water permeability for cracks above 100 microns ranged between mortar and normal strength concrete.

ACKNOWLEDGEMENTS

This research was carried out at the ACBM Center, Northwestern University. Support from the National Science Foundation (NSF) through grant DMS/9313013 to the National Institute of Statistical Sciences (NISS) is greatly appreciated.

REFERENCES

- [1] Aldea, C., Shah, S.P., Karr, A., Permeability of Cracked Concrete (submitted to publication).
- [2]. Wang, K., Jansen, D., Shah, S.P., Karr, A., Permeability study of cracked concrete, *Cement and Concrete Research*, Vol. 27, No. 3, pp. 381-393, 1997.
- [3]. Ludirdja, D., Berger, R. L., Young, F., Simple Method for Measuring Water Permeability of Concrete, *ACI Materials Journal*, Vol. 86, No. 5, September-October, pp. 433-439, 1990.
- [4]. Gérard, B., Breysse, D., Ammouche, A., Houdusse, O., Didry, O., Cracking and Permeability of Concrete Under Tension, *Materials and Structures*, Vol. 29, April, pp. 141-151, 1996.
- [5]. Gérard, B., Marchand, J., Breysse, D., Ammouche, A., Constitutive Law of High-Performance Concrete Under Tensile Strain, 4th International Symposium on Utilization of High-Strength/High-performance Concrete, Paris, 1996.
- [6]. Standard Test Method for Electrical Indication of Concrete's Ability to Resist Chloride Ion Penetration, Designation C 1202 – 94, *Annual Book of ASTM Standards*, Vol. 04.02, pp. 620-625.
- [7]. Castro-Montero A., Jia Z., Shah S.P., Evaluation of Damage in Brazilian test Using Holographic Interferometry, *ACI Materials Journal*, vol. 92, No. 3, May-June, pp.268-275, 1995.
- [8]. Gettu, R., Mobasher, S., Carmona, S., Jansen, D., Testing of Concrete Under Closed-Loop Control, *Advanced Cement-Based Materials*, Vol. 3, No. 2, pp.54-71, 1996.
- [9]. Hearn, N., *Saturated Permeability of Concrete as Influenced by Cracking and Self-sealing*, Ph. D. Thesis, University of Cambridge, p. 229, 1992.
- [10] Hearn, N., Morley, C.T., Self-sealing property of concrete – Experimental evidence, *Materials and Structures*, vol. 30, August-September, pp. 404-411, 1997.
- [11]. Ruettgers, A., Vidal, E. N., Wing, S. P., An Investigation of the Permeability of Mass Concrete with particular Reference to Boulder Dam, *Journal of the American Concrete Institute – Proceedings*, March-April, pp. 382-416, 1935.

- [12]. Cernica, J. N., *Geotechnical Engineering: Soil Mechanics*, John Wiley & Sons, Inc., p. 125, 1995.

Table 1. Details of test series and mixture proportions.

Mixture Ingredients	Weight by mc of material (kg)			
	PASTE	MORTAR	NSC	HSC
Cement	325.59	155.87	81.91	114.64
Coarse Aggregate (#4)	-	-	304.01	286.33
Fine Aggregate	-	253.06	132.54	122.71
Water added	146.51	95.88	50.37	25.85
Silica Fume (slurry)	-	-	-	29.20
Superplasticizer (suspension)	-	-	-	3.35
W/C	0.45	0.45	0.45	0.31

Note: the amounts of silica fume and superplasticizer presented in the table contain 50% and respectively 60% water by weight.

Table 2. Material Properties.

Material Properties	Material Type			
	PASTE	MORTAR	NSC	HSC
Slump (cm)	-	-	7.5	1.8
Modulus od Elasticity* (GPa)	12.37	18.57	32.14	19.12
Tensile Strength* (MPa)	1.57	4.25	3.84	5.69
Compressive Strength* (MPa)	55	33	36	69

Note: * measured at 28 days.

Table 3. Cracking and Material Effect on Permeability Coefficient, 25 mm Samples.

Material Type	Uncracked	Cracked (~ 100 microns)	
	Permeability coefficient, k (cm/s)	COD after unloading (microns)	Permeability Coefficient, k (cm/s)
PASTE	6.00×10^{-9}	113	3.51×10^{-7}
MORTAR	2.58×10^{-9}	129	3.11×10^{-8}
NSC	1.39×10^{-9}	131	2.08×10^{-8}
HSC	3.90×10^{-10}	110	3.39×10^{-8}

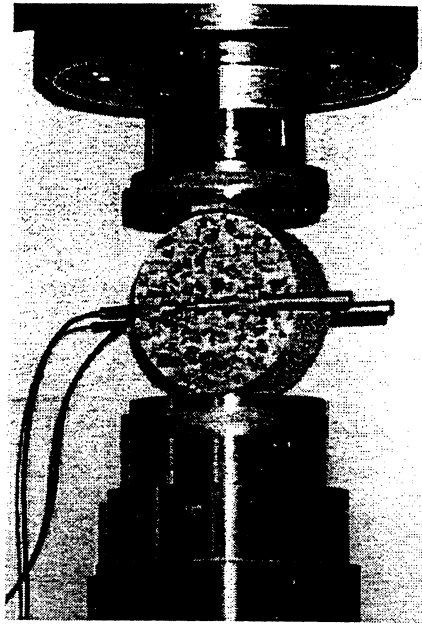


Fig. 1. Splitting tensile test setup.

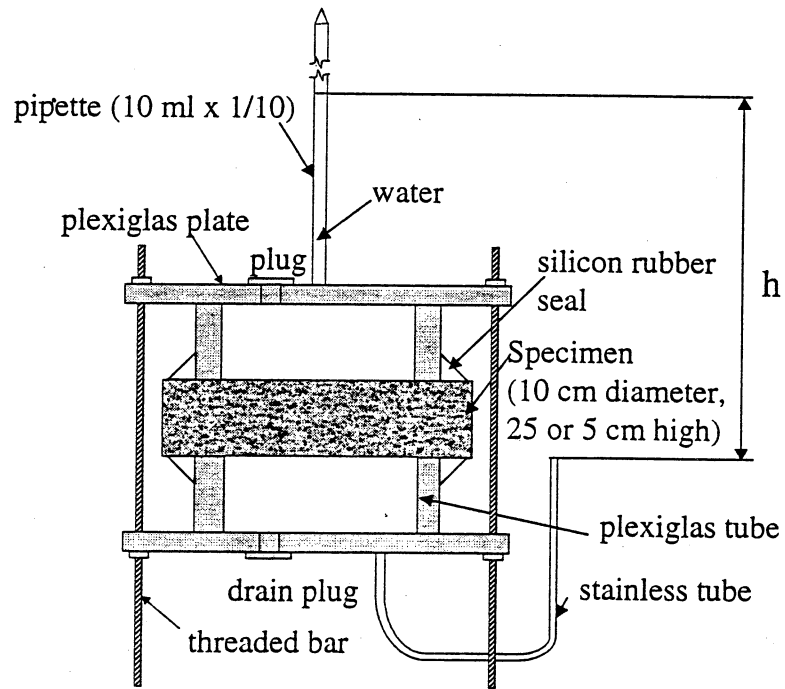


Fig. 2. Water permeability test setup.

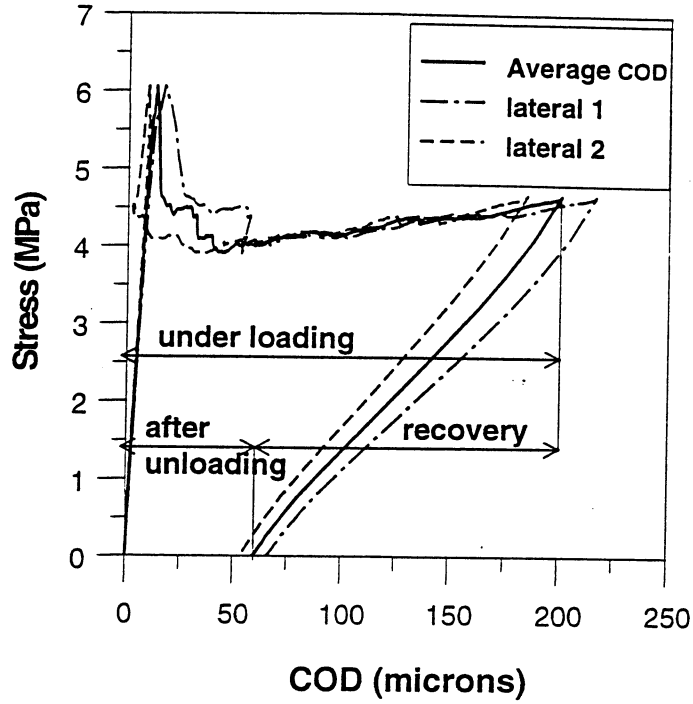


Fig. 3. Typical splitting tensile test stress-COD curve.
HSC, COD 200 microns.

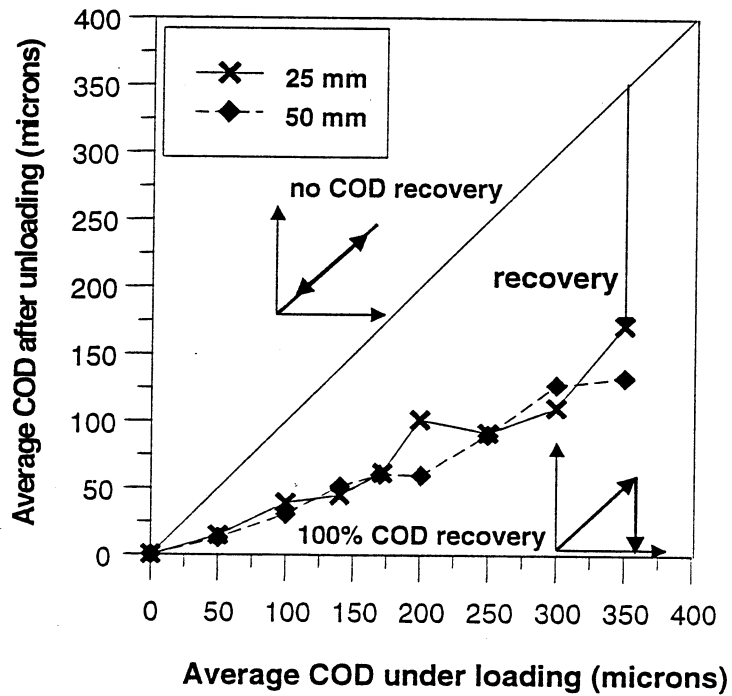


Fig 4. Recovery of COD after unloading.
HSC, thickness effect.

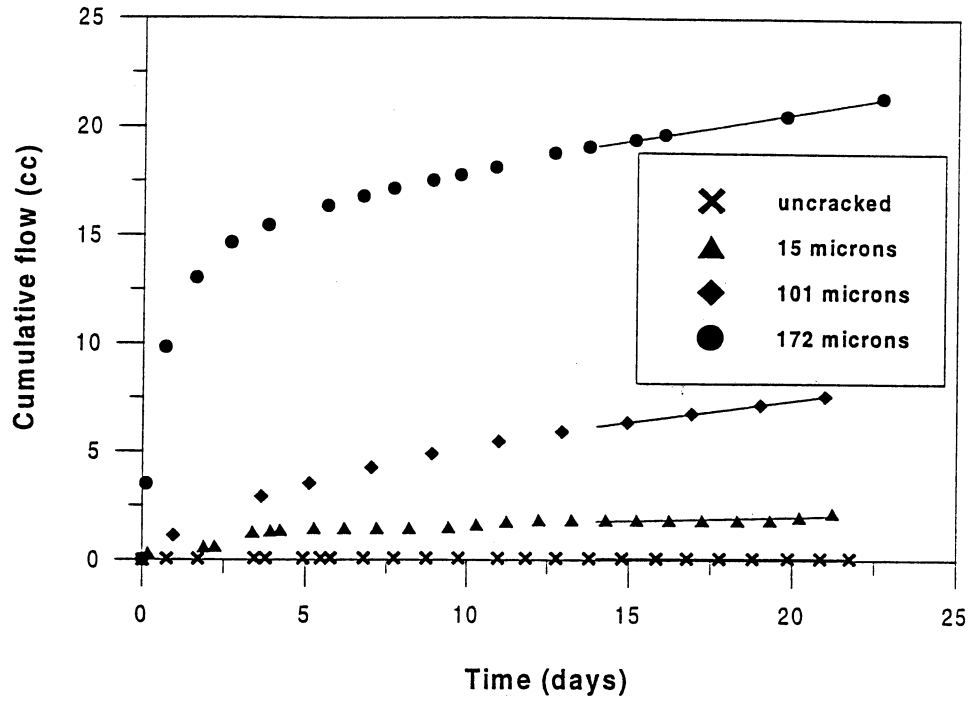


Fig. 5. Dependence of cumulative flow with cracking, HSC, 25 mm.

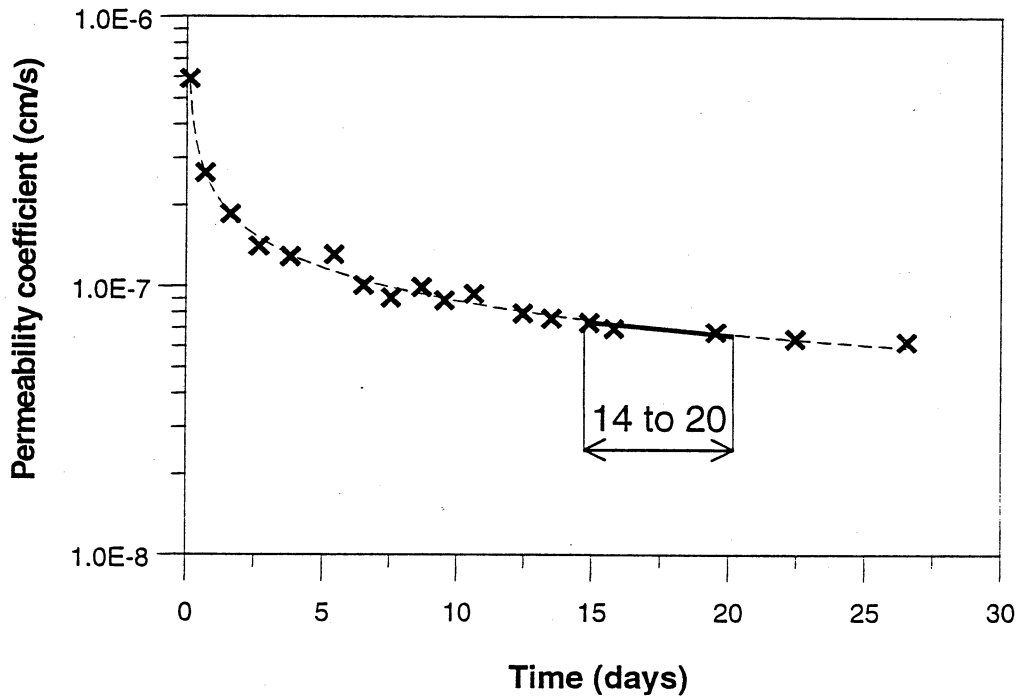


Fig. 6. Typical permeability coefficient curve in time. HSC, 50 mm, COD 127 microns.

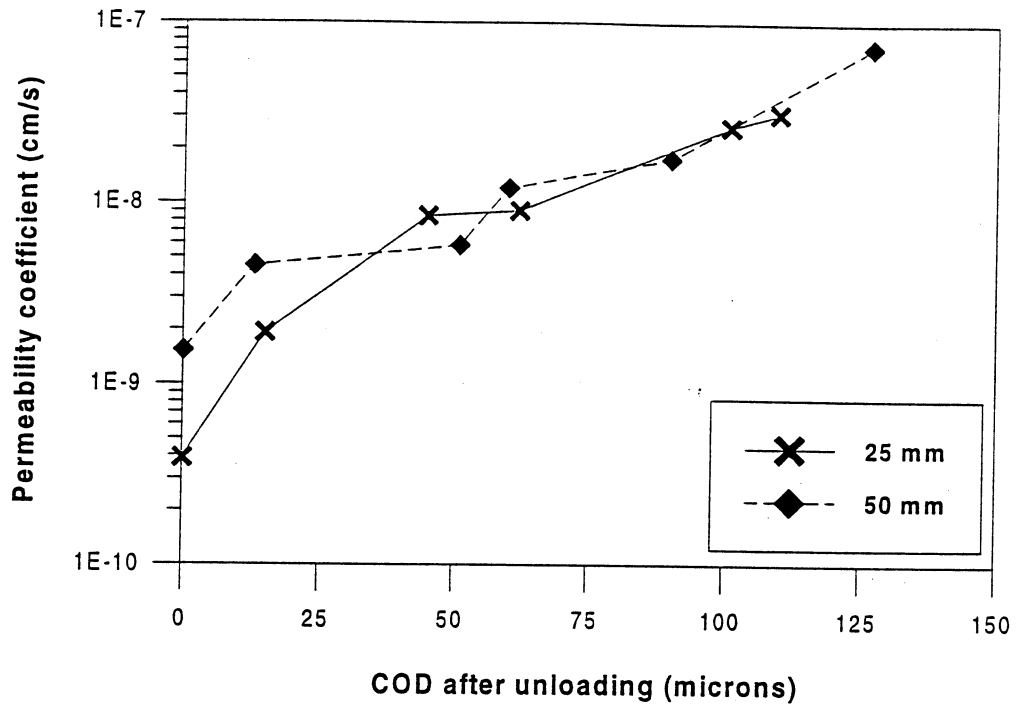


Fig. 7. Thickness effect on permeability, HSC.

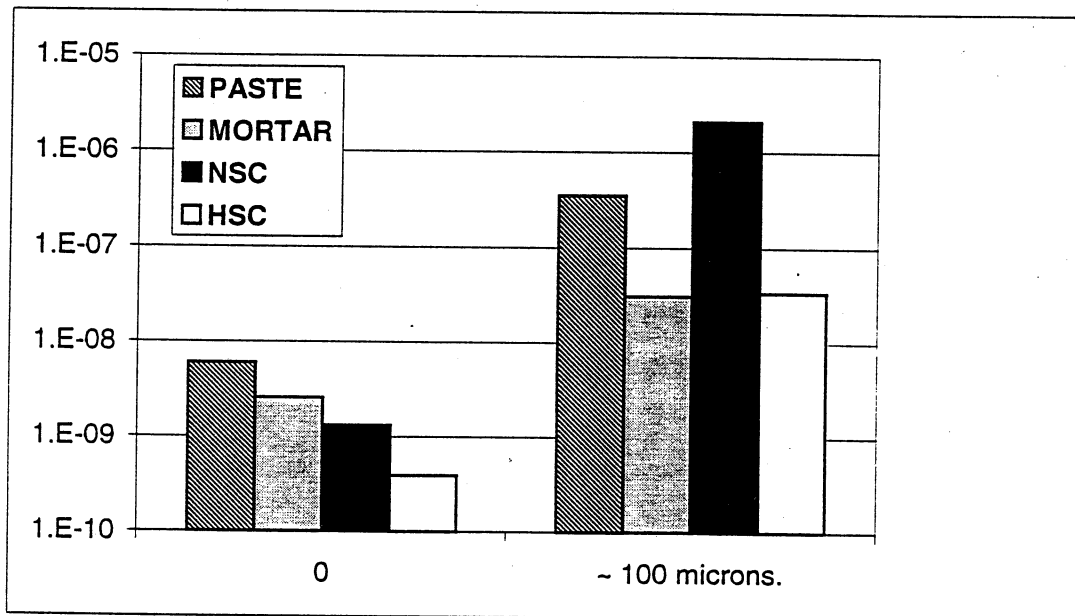


Fig. 8. Material effect on permeability, 25 mm samples.

LIST OF TABLES

- Table 1 Details of test series and mixture proportions.
- Table 2. Material properties.
- Table 3 Cracking and material effect on permeability coefficient, 25 mm samples.

LIST OF FIGURES

- Fig. 1. Splitting tensile test setup.
- Fig. 2. Water permeability test setup.
- Fig. 3. Typical splitting tensile test stress-COD curve. HSC, COD 200 microns.
- Fig. 4. Recovery of COD after unloading. HSC, thickness effect.
- Fig. 5. Dependence of cumulative flow with cracking, HSC, 25 mm.
- Fig. 6. Typical permeability coefficient curve in time. HSC, 50 mm, COD 127 microns.
- Fig. 7. Thickness effect on permeability, HSC.
- Fig. 8. Material effect on permeability, 25 mm samples.